Available online at www.sciencedirect.com
SCIENCE DIRECT
Polymer 46 (2005) 1851–1856
polymer
www.elsevier.com/locate/polymer

Poly(methylmethacrylate)-silica nanocomposites films from surface-functionalized silica nanoparticles

Ying-Ling Liu*, Chih-Yuan Hsu, Keh-Ying Hsu

Department of Chemical Engineering and R&D Center for Membrane Technology, Chung Yuan Christian University, Chungli, Taoyuan 320, Taiwan, ROC

Received 17 September 2004
Available online 19 January 2005

Abstract

Poly(methylmethacrylate)-silica nanocomposite films were prepared from copolymerizing methylmethacrylate with allylglycidylether-functionalized silica nanoparticles. No alkoxysilane coupling agents and sol–gel reactions were employed in this preparation approach to result in nanocomopsite films having silica contents higher than 70 wt%. Good transparency, hardness above 9H grade, and superior surface planarity were observed with the prepared naocomposite films. Glass transition temperatures were not observed with the nanocomposite films by DSC measurement to indicate their good thermal and dimensional stability.

Keywords: Poly(methylmethacrylate); Silica; Nanocomposite films

1. Introduction

Polymer-silica nanocomposite materials [1–2] received wide attention of researches for their attractive properties to be potentially applied in protective coatings, high refractive index films, optical waveguide materials, and flame retardants [3–6]. Among the nanocomposite materials, one of the most widely studied is poly(methyl methacrylate)-silica nanocomposite materials [7–13]. The sol–gel process with using alkoxysilane compounds as precursors was commonly utilized in preparing PMMA-silica nanocomposite materials. However, owing to the poor thermal stability of PMMA, the curing temperature of the nanocomposite materials was limited, so as to result in an incomplete condensation of Si–OH groups. The residual Si–OH groups in the nanocomposite materials obtained showed significant harms to the optical and thermal properties of the PMMA-silica nanocomposite materials. To overcome this problem, preformed nanosized colloidal silica was used to prepare PMMA-silica nanocomposite materials [12–14]. Kashiwagi et al. [13] disclosed the preparation of PMMA-silica nanocomposites from in situ polymerization of MMA together with silica nanoparticles. Homogeneous dispersion of the silica particles in the PMMA matrix was found. However, there were not covalent linkages between the organic and inorganic domains to reduce the glass transition temperature of the nanocomposites. To introduce chemical bonding between the PMMA chains and silica particles, Yu et al. [14] used 3-(trimethoxysilyl)propyl methacrylate to modify the silica surface, and then copolymerized the modified silica particles with MMA. A post curing process was applied to promote the conversion of the silanol dehydration reactions. In Yu's work covalent linkages were introduced to promote the miscibility between organic and inorganic domains. However, sol–gel reaction was still involved in preparing nanocomposite materials to reduce the thermal stability of the resulted products.

Here, allylglycidylether (AGE) was utilized as a surface modifier for silica nanoparticles [15]. The AGE-modified silica particles were then copolymerized with MMA to form PMMA-silica nanocomosite films. This approach introduced covalent bonds between PMMA and silica particles and did not employ alkoxysilane compounds and sol–gel process in the preparation process, consequently to overcome the drawbacks found in the reported literatures. Transparent PMMA films having very high silica contents, superior thermal

[* Corresponding author. Tel.: +886 3 2654130; fax: +886 3 2654199.
E-mail address: ylliu@cycu.edu.tw (Y.-L. Liu).

0032-3861/$ - see front matter © 2005 Elsevier Ltd. All rights reserved.
doi:10.1016/j.polymer.2005.01.009

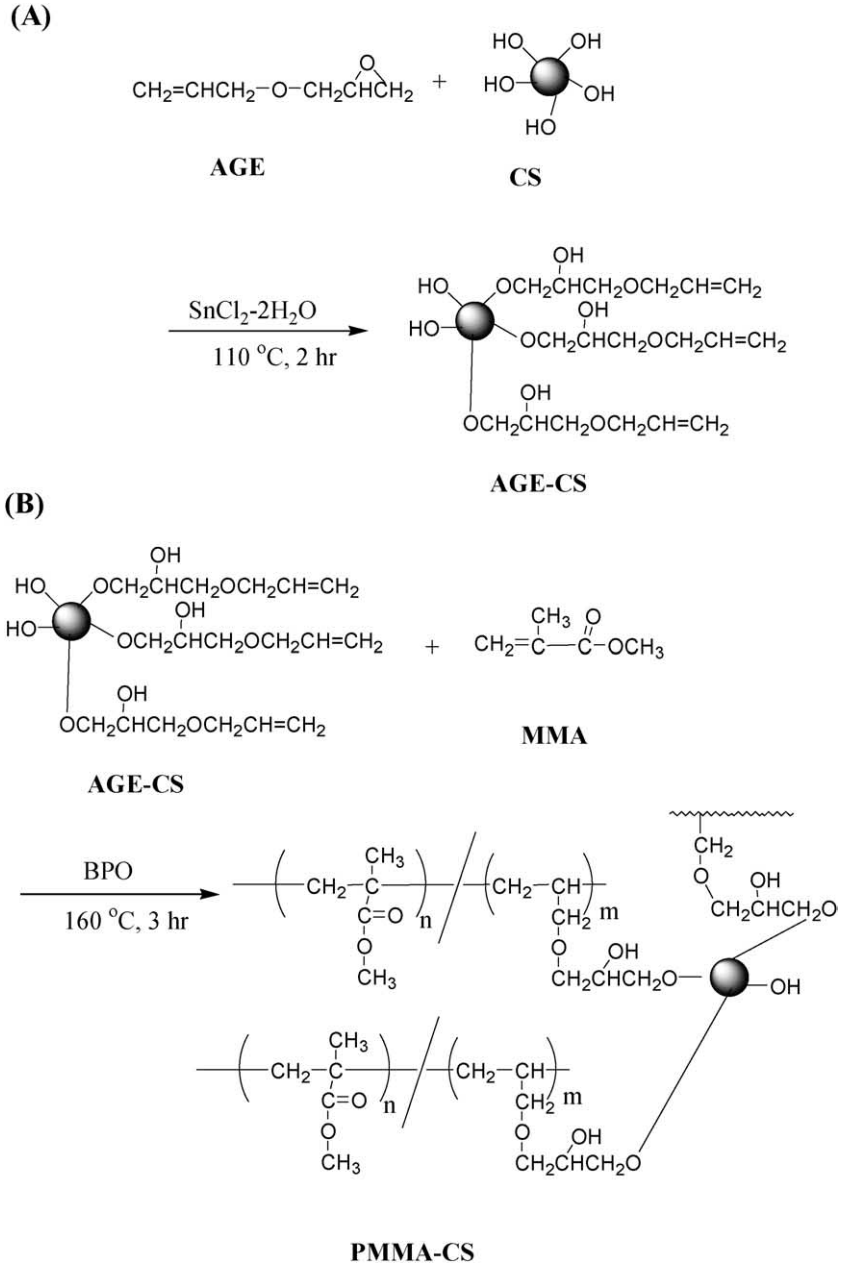

Fig. 1. Preparation of AGE-CS and PMMA-CS nanocomposite materials

stability, low surface roughness, and high hardness were obtained.

2. Experimental

2.1. Materials

Nanoscale silica particles (CS) were purchased from Nissan Chemical Co., Japan. The commercial product of MIBK-ST, in which 30–31 wt% of silica (particle size: 10–20 nm) was dispersed in methylisobutylketone (MIBK), was used. Allylglycidylether (AGE) and methylmethacrylate (MMA) from Aldrich Co. were used as received. The AGE modified silica particles (AGE-CS) were prepared through reacting AGE with silica particles according to the reported method [15]. The reaction composition in weight ratio was 20/80 of AGE/CS. The characterization on AGE-CS with FTIR, ^{1}H NMR, EDX and TEM reported in the previous work [15] gave sufficient support to the desired structure of AGE-CS as shown in Fig. 1. The grafting ratio of AGE in AGE-CS is ca. 0.35 mmol/g. Benzylperoxide (BPO) purchased from Aldrich Co. was used as an initiator of MMA polymerization.

Table 1
Preparation of PMMA-CS nanocomposite materials

PMM-A-CS	MMA (g)	Molar ratios of MMA/AGE in feeding monomers	Silica content in nanocomposite film (wt%)
HM-40	4.5	4.24	43
HM-50	3.0	2.83	50
HM-60	2.0	1.89	63
HM-70	1.3	1.23	70
HM-80	1.25	0.71	76

2.2. Characterization

FTIR spectra were measured with a Perkin Elmer spectrum one FTIR. Differential scanning calorimetry thermograms were recorded with a Thermal Analysis (TA) DSC-Q10 in a nitrogen gas flow of 40 mL/min. Thermogravimetric analysis (TGA) was performed by a TA TGA-2050 at a heating rate of 10 °C/min under nitrogen or air atmosphere. The gas flow rate was 100 mL/min. Scanning electron micrographs were observed with a Hitachi S-3000N Hi-SEM. Energy dispersive X-ray (EDX) measurements were conducted with a Horiba ES-320 Energy Dispersive X-Ray Micro Analyzer. Atomic force microscopy (AFM) measurements were carried out with an AFM of Seiko SPI3800N, series SPA-400. Elemental analysis was measured with a Heraeus CHN-O rapid elementary analyzer with benzoic acid as a standard. The hardness of the nanocomposite material films was measured by using a pencil test.

2.3. Preparation of PMMA-CS nanocomposite materials

Certain amounts of AGE-CS and MMA monomer dissolved in 60 mL of THF were added BPO (0.5 g) with stirring. The reaction mixture was degassed for three times and then reacted at 60 °C for 3 h under nitrogen atmosphere. After cooling the solution was cast on a glass substrate and then dried under vacuum at 80 °C for 12 h. The reaction compositions were collected in Table 1.

3. Results and discussion

The polymerization of MMA with AGE-CS was successfully performed through the conventional free-radical polymerization process (Fig. 1). After the reaction, an increase in viscosity of the reaction solution was observed. All of the reaction solutions were transparency and precipitation and gel phenomena did not occur during the polymerization. The PMMA-silica nanocomposite films were obtained from spinning-coating the solution on a glass plate. The chemical compositions of the nanocomposite materials were determined by elemental analysis. The silica contents of the nanocomposite calculated from the elemental analysis data were listed in Table 1. Excepting HM-80, all of the nanocomposite materials exhibited high transparency to indicate the homogeneous dispersion of the silica particles in the PMMA polymers. The good compatibility and homogeneous dispersion of the silica nanoparticles with PMMA were noteworthy. The somewhat opaque appearance of HM-80 might be due to its high silica content. A phase inversion of the organic and inorganic phases occurred for HM-80, i.e. the silica domain becoming the continuous phase and the PMMA domain the dispersing phase. The high silica contents of the HM films also indicated that using surface-modified silica to copolymerize with MMA could significantly improve the preparation performance of polymer-silica nanocomposites, since PMMA-silica nanocomposite materials having such high silica contents have not ever been reported [12–14]. Incorporation of the high silica contents to PMMA also significantly enhanced the hardness of the nanocomposite films. With a pencil test all of the samples showed hardness above grade of 9H.

Fig. 2 showed the SEM and EDX Si-mapping photography of HM-50. From the SEM photography aggregation of silica was not observed. The fracture surface was very dense. Both of the SEM and EDX Si-mapping results indicated the homogeneous dispersion of the silica in the polymer matrix. The dispersion of the silica particles in the PMMA matrix was also observed with TEM. As it can be

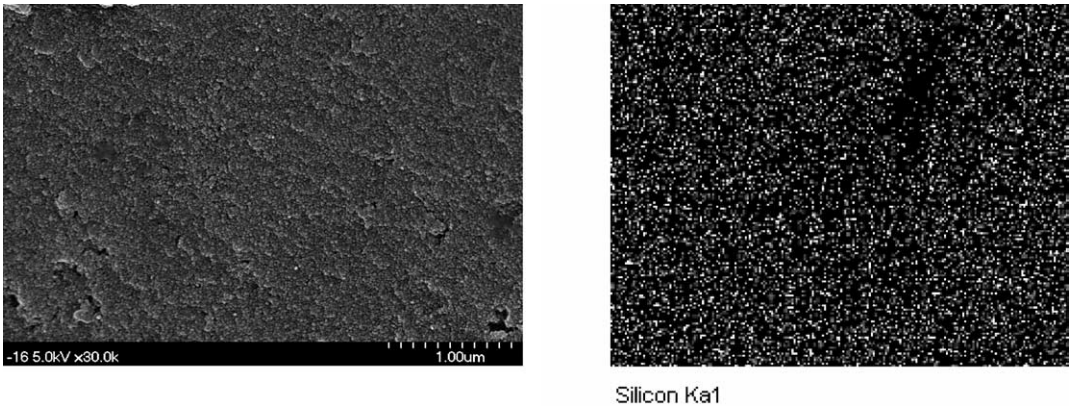

Fig. 2. SEM (left) and EDX-Si mapping (right) microphotographs of HM-50.

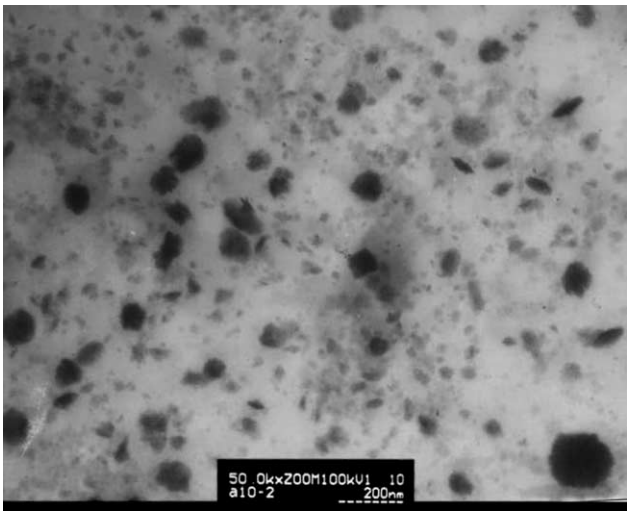

Fig. 3. TEM microphotographs of HM-50.

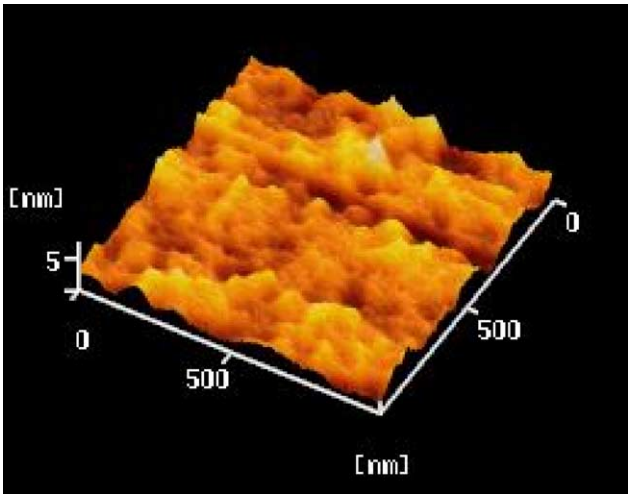

Fig. 4. AFM micrograph of HM-50 for measuring its surface planarity.

seen in Fig. 3 most silica particles had size of about 10–20 nm. However, some silica clusters ranging from 50–80 nm were observed. Since the particle sizes of AGE-CS were analyzed to be similar to the pristine MIBK-ST, which showed a distribution of two groups of about 8–10 nm and 40–60 nm [16], from the TEM micrograph it was concluded that particle arrogation did not occur during polymerization and film formation. On the other hand, Fig. 4 showed the typical AFM micrograph of HM-50. The average roughness and root mean square roughness were found to be 6.4 and 8.2 Å, respectively. The low surface roughness of the prepared film was noteworthy, as a roughness of about 30 Å was reported for PMMA/silica nanocomposite film having similar 50 wt% of silica content [14]. It was concluded that the planarity of the PMMA/silica nanocomposite film could be significantly improved with using the surface-functionalized silica.

The thermal properties of the nanocomposite materials were evaluated with DSC and TGA. Fig. 5 showed the DSC thermograms of PMMA and the nanocomposite materials. Only pure PMMA showed a glass transition temperature (T_g) at about 115 °C. For all of the nanocomposite films, glass transition behavior was not observed with DSC (Thermal analysis TA DSC-Q10) measurements till 250 °C [13]. The glass transition behavior of the nanocomposite materials were also not observed by a thermal mechanical analyzer (TMA, Perkin Elmer TMA-7). The disappearance of T_g implied the motion of the PMMA chains were seriously restricted by the silica particles. The restriction could be also coming from the crosslinking bonding between PMMA chains and silica particles [14], since a decrease in T_g was observed with the PMMA-silica nanocomposite materials which have not inter-phase bonding [13].

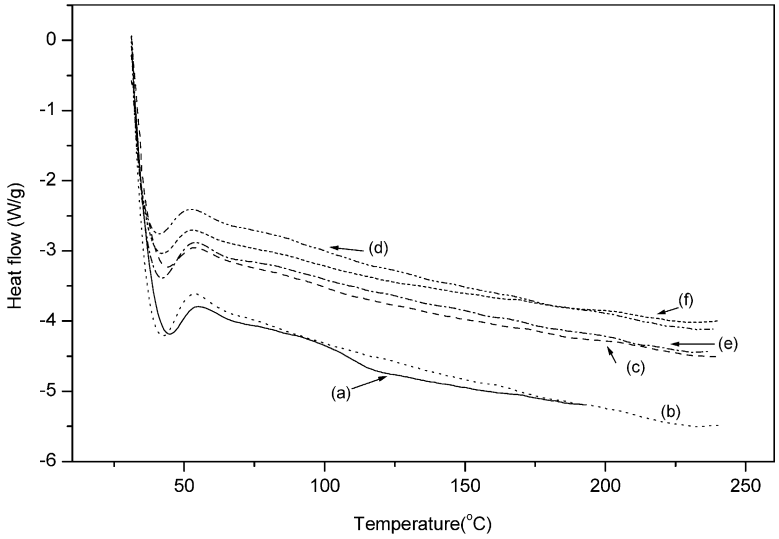

Fig. 5. DSC thermograms of PMMA and its nanocomposite materials: (a) PMMA, (b) HM-40, (c) HM-50, (d) HM-60, (e) HM-70, and (f) HM-80.

Table 2
Thermal degradation data of PMMA and the nanocomposite materials in nitrogen

Sample	Degradation temperatures (°C)			Char yield (wt%)	Calculated silica content (wt%)
	Head-to-head structure	Unsaturated end	Polymer backbone		
PMMA	165, 212	296	401	0	0
HM-40	177	296	388	39	43
HM-50	174	299	395	49	50
HM-60	177	297	388	60	63
HM-70	179	294	378	69	70
HM-80	180	299	378	75	76

Fig. 6 showed the TGA and DTG thermograms of PMMA and its nanocomposite films heated in nitrogen. While being compared with PMMA, the HM films showed high temperatures of 10% weight loss (T_d). An increase of T_d was generally considered as an indication of enhancement on thermal stability [14]. On the other hand, since the inorganic part (silica) of the nanocomposite films almost did not lose its weight during the heating period, the shift of T_d to high temperature region might be simply due to that the nanocomposite films possessed relatively small amount of

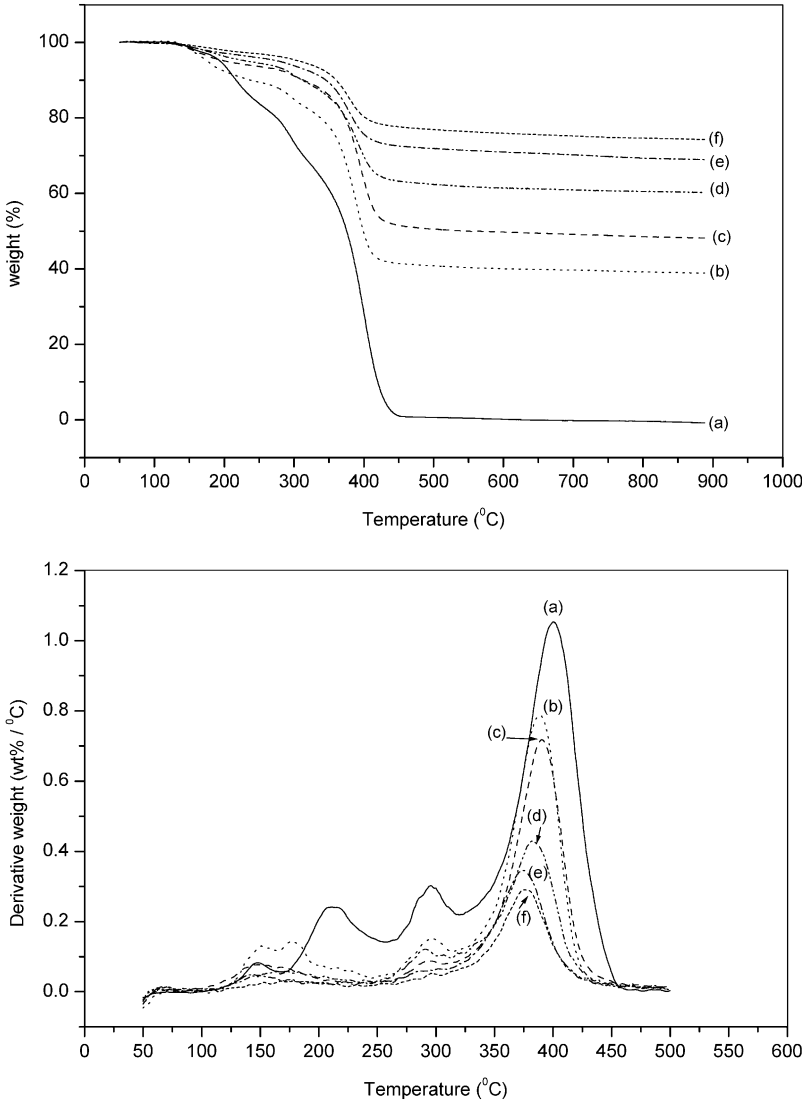

Fig. 6. TGA (upper) and DTG (lower) thermograms of PMMA and its nanocomposite materials: (a) PMMA, (b) HM-40, (c) HM-50, (d) HM-60, (e) HM-70, and (f) HM-80.

organic polymer, which contributed to the weight loss. According to previous reports, addition of nanosilica particles into a polymer did not significantly altered the thermal degradation mechanism of the polymer part of a polymer-silica nanocomposite material [6,13]. Similar behavior was also observed in this study with PMMA-silica nanocomposite films. As it can be seen in the DTG thermograms, pure PMMA showed a 4-staged degradation mechanism (Table 2). It is known that radical polymerization PMMA starts to degrade by initiation at the head-to-head linkages at around 160 °C. It was also reported that for PMMA oligomer the head-to-head degradation might initiate at about 195 °C [17]. Therefore, the first two stages of weight loss for the pure PMMA might be from the degradation of head-to-head linkage. However, the first weight loss might also be possibly from the residual solvent and/or MMA monomer in the polymer. The last two stages of weight loss were corresponding to the degradation initiating at the unsaturated ends (at about 296 °C) and at the polymer backbones (at about 400 °C). Similar degradation patterns were also observed with the PMMA nanocomposite films. The degradation temperatures of each stage were collected in Table 2. From the DTG data it was concluded that incorporation of nanosilica particles into the PMMA polymer did not change the degradation mechanisms of the polymer. That is to say, the thermal stability of PMMA was not enhanced with the addition of silica particles.

Since the degradation patterns of the nanocomposite films were similar to that of PMMA, all of the weight loss of the nanocomposite films should only come from the degradation of PMMA. The coincidence between the silica contents and the char yields of the nanocomposite films also support this viewpoint (Table 2). This conclusion agreed with the result reported by Kashiwagi et al. [13], but was different from Yu's work [14]. This is because that alkoxysilane compounds and sol-gel process were employed in Yu's work. Silica network formed from sol–gel reaction might penetrate into the PMMA chains, consequently to form a barrier layer to retard the degradation of the polymer domain and to enhance the thermals stability of the polymer char, therefore to increase the char yields [18–19]. However, the above effect did not work for nanocomposites films prepared from preformed silica particles, as being observed in Kashiwagi's report [13] and this work.

4. Conclusion

It was concluded that the covalent bond linkages between the inorganic silica and organic PMMA polymer provided extreme high compatibility of these two domains to result in the high silica contents (over 70 wt%) of the nanocomposite materials. The prepared nanocomposite films exhibited extremely high hardness, surface planarity, and good thermal stability. On the other hand, incorporation of the silica particles did not altered the thermal degradation behaviors of PMMA.

Acknowledgements

Financial support on this work from the Ministry of Economic Affairs of Taiwan is highly appreciated. The authors also thank Prof. R.-J. Jeng at National Chung Hsing University (Taichung, Taiwan) for his kind help in AFM measurements.

References

[1] Mark JE, Lee CYC, Bianconi PA, editors. Nanocomposite organic-inorganic composites, ACS Sym. Ser. 585. Washington DC: American Chemical Society; 1995.
[2] Laine RM, Sanchez C, Brinker CJ, Giannelis E, editors. Organic/inorganic nanocomposite materials, Vol. 628. Warrendale, PA: Materials Research Society; 2000.
[3] Erashad-Langroudi A, Mai C, Vigier G, Vassoille R. J Appl Polym Sci 1997;65:2387.
[4] Lee LH, Chen WC. Chem Mater 2000;13:137.
[5] Yashida M, Prasad PN. Chem Mater 1996;8:235.
[6] Liu YL, Hsu CY, Wei WL, Jeng RJ. Polymer 2003;44:5159.
[7] Wang YT, Chang TC, Hong YS, Chen HB. Thermochim Acta 2003; 397:219.
[8] Huang ZH, Qiu KY. Polymer 1997;38:521.
[9] Chen WC, Lee SJ. Polym J 2000;32:67.
[10] Soloukhin VA, Posthumus W, Brokken-Zijp JCM, Loos J, With G. Polymer 2002;43:6169.
[11] Yang F, Yngard RA, Nelson GL. Proceedings of nanocomposites 2002-delivering new value to polymers, San Diego CA 2002.
[12] Yang F, Nelson GL. J Appl Polym Sci 2004;91:3844.
[13] Kashiwagi T, Morgan AB, Antonucci JM, VanLandingham MR, Harris RH, Awad WH, et al. J Appl Polym Sci 2003;89:2072.
[14] Yu YY, Chen CY, Chen WC. Polymer 2003;44:593.
[15] Liu YL, Hsu CY, Wang ML, Chen HS. Nanotechnology 2003;14:13.
[16] Liu YL, Li SH. Macromol Rapid Commun 2004;25:1392.
[17] Cacioii P, Moad G, Rizzardo E, Serelis AK, Solomon DH. Polym Bull 1984;11:325.
[18] Liu YL, Wu CS, Chiu YS, Ho WH. J Polym Sci Part A: Polym Chem 2003;41:2354.
[19] Hsiue GH, Liu YL, Tsiao J. J Polym Sci Part A: Polym Chem 2001; 39:986.